RESEARCH ARTICLE OPEN ACCESS

Fracture Toughness Characterization

Manuel Beltrán Z.*, Felipe Hernández S.*, Diego Rivas L**, Jorge L. González V**, Héctor Dorantes R.**
*(Sección de Estudios de Posgrado e Investigación/ Escuela Superior de Ingeniería Mecánica y Eléctrica Unidad Azcapotzalco/ Instituto Politécnico Nacional, México D.F)
** (Departamento de Ingeniería en Metalurgia y Materiales/ Escuela Superior de Ingeniería Química e Industrias Extractivas/ Instituto Politécnico Nacional, México D.F.)

ABSTRACT
This paper addresses the fracture toughness (K_{IC}), or also known as critical stress intensity Factor, according to conditions of Lineal Elastic Fracture Mechanics (LEFM). The characterization of the mechanical properties in tensile and fracture toughness of structural steel pipes API-5L used in hydrocarbons transportation was performed. For fracture toughness, the material was tested through fatigue crack propagation on standardized compact specimen (CT) according to ASTM E-399 norm. A thickness (B) equal to $\frac{w}{4}$ and a crack size (a) equal to 0.5*w* were used. With the porpoise of establishing the adequate conditions at the crack tip, the specimens were subjected to fatigue pre-cracking by application of repeated cycles of load in tensile-tensile and constant load amplitude with a load ratio of R = 0.1. The experimental Compliance method was used based on data obtained from load vs. Crack Mouth Opening Displacement (CMOD). The results show a Stress Intensity factor of 35.88 MPa√m for a 25 mm crack size specimen. The device used for testing is a MTS-810 machine with capacity of 100KN and 6 kHz sampling rate, which meets the conditions of the ASTM E-399 standard. The cracking susceptibility of steel is influenced by the size, morphology and distribution of non-metallic inclusions, thermochemical interaction with the environment and microstructure.
Keywords – Fracture Toughness, Fracture Mechanics, Crack, Finite Element Method, Stress Intensity Factor.

I. INTRODUCTION

The traditional design criteria idealize the mechanical properties of the materials, considering it as homogeneous, lineal, isotropic and free of defects. Generally, the materials contain microscopic defects generated by the manufacturing conditions, by environment reactions or generated during service. The use of metal components in structures such as bridges, aircrafts, pipelines, buildings, cars, etc, always is accompanied by the risk of fracture, so the unexpected failure of these large structures occurs, usually followed by enormous human, economic and material loss. Failure by fracture is associated to poor quality of the product or defects in design, so in addition to de direct losses from the failure of the element, also must be considered losses by production delay, environment damage, and the deterioration of the image of the company to the public opinion.

In real conditions, defects, particularly cracks, are present in mechanical components and structures. That is the major reason to analyze its effect on the component performance before the defect grows until a critic size to propagate catastrophically [1].

In particular, the susceptibility to cracking of steel is influenced by size, morphology and distribution of nonmetallic inclusions, thermochemical interaction to the environment and microstructural properties [2].

For these reasons, was developed the fracture mechanics science which has adopted a significant role in the failure analysis field. It is a discipline that provides the basis and methodology for design and evaluate the cracked components to determine if the crack size is dangerous, in order to develop stronger structures, admit defect's tolerances and predict the residual life of the element.

There is an important interest in studying the crack propagation in structural materials. This study assume the basis of fracture mechanics science to determine the crack propagation rate, stress intensity factor and other material properties in order to stablish the crack propagation conditions. Previous work determined the stress intensity behavior at the crack tip [3] Irwin described the stress magnitude present in each one of the three fracture modes. Paris et al. [4] found a model to describe the stress field at the crack tip using a two dimensional loading model to describe the stress magnitude in this region assuming the material behaves in a linear elastic manner. In 1961, Paris et al. [5] they published "a critical analysis of crack propagation laws" that evaluates the laws presented by Mc Evily's [6], Liu's [7] and Dugdale's [8] works to stablish the similitudes and contradictions of these studies.

In this work the tensile and fracture toughness properties were evaluated in structural steel API-5L at different rolling orientations. The norm ASTM E-399 [9] was adopted for stablish the stress intensity

factor using compact specimens. The specimens were tested applying repeated load cycles in tensile-tensile range and constant load amplitude at room temperature and constant humidity. Also, a microstructural analysis was performed.

II. EXPERIMENTAL PROCEDURE

2.1 Cracking Plane

According to ASTM E-399 norm, three crack propagation directions are considered. In particular case of tubes and cylinders, the longitudinal direction (L) is parallel to axial axis, Circumferential (C) direction propagates around the perimeter and finally, the radial direction (R) propagates across the material thickness.

2.2 Specimen Geometry

The specimens were made according to ASTM E-399 norm. The figure 1 shows the compact specimen geometry where a parameter "w" determines the thickness (B) of the specimen with the ratio $2 \leq (w/B) \leq 4$.

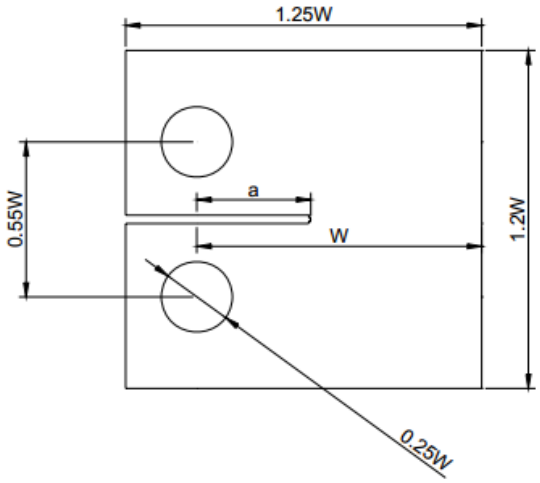

Fig. 1. Compact Specimen geometry. ASTM E-399.

In this geometry, a simulated crack is introduced by manufacturing a notch with a depth between $0.45 \leq (a/w) \leq 0.55$.

2.3 Fatigue Precracking

In order to stablish the appropriate characteristics in the crack tip, the specimens should be precracked in the finally heat treatment conditions. The load amplitude at first step will be described by the equation $\frac{K_{max}}{E} = 0.00013\sqrt{m}$ and the finally step would be taken as $\frac{K_{max}}{E} = 0.0001\sqrt{m}$ and the load ratio (R) equal to 0.1. Pre-cracking extension must be done between 1.3 and 1.5 mm [10]

2.4 Fracture Toughness Test

The tests were performed at room temperature using the compliance method. In this method, the applied load (P) and Crack Opening Displacement (√) are recorded. The load ratio used was R=0.1 in tensile-tensile range of cyclic load and 15 Hz frequency. The Crack opening displacement was recorded using an extensometer mounted at the notch edges located at the point V_0 according to ASTM E-647 [11]. The figure 2 shows the specimen and extensometer mounting. Although, a traveler telescope and a dial micrometer are aligned to observe the crack extension.

Fig. 2. Specimen and extensometer mounting.

2.5 Finite Element Analysis

Simultaneously, a finite element analysis was performed using Ansys Multiphysics 14.5 software. A compact specimen (CT) was simulated in a 3D model according to geometry and sizing of the experimental specimens in order to compare the testing results with simulation values. The specimen was loaded in the load axis by 13 kN tensile strength in opposite directions. The meshing used in the analysis was characterized by a maximum element separation of 1 mm. The tetrahedral meshing method was used accompanied of tet10 element. The figure 3 indicates the meshing in finite element analysis.

The generated meshing contains 162748 elements and 232679 nodes in tetrahedral form. The asymmetry average obtained was 0.2309 that is considered inside an excellent degree according to software auto evaluation.

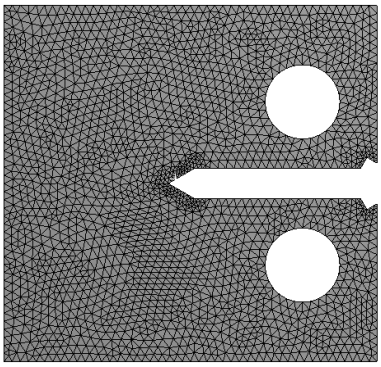

Fig. 3. Compact specimen meshing.

Because of the presence of a wide stress gradient's in a small zone around the crack tip. A refinement was realized in the proximity of the crack tip's edges to evaluate properly the stress concentration and strain in this zone. Figure 4 shows the refinement meshing.

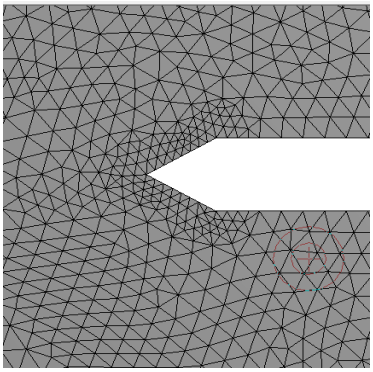

Fig. 4. Refinement meshing at the Crack tip.

The material properties would be assumed as the same as the mechanical characterization results.

2.6 Apparatus

The apparatus used to realize this test were a servo hydraulic machine MTS-810 with load capacity of 100 KN and a MTS extensometer 632.O3F-40 with initial opening of 6mm. The crack opening extension should be monitoring by a traveler telescope and a dial micrometer aligned with the MTS-810 by a worm device at the specimen front pointing the crack tip to follow its extension.

III. RESULTS

3.1 Chemical Analysis

The chemical characterization was realized by spectroscopy atomic emission with a spectrolab 2007. The test was realized by three shoots in a polished area of the material. Table I shows the results obtained. An average content of carbon of 0.235 was determined.

Direction	E MPa	σ_0 MPa	σ_{UTS} MPa	% ε
L_{Std}	$180x10^3$	394	521	28
C_{Std}	$202x10^3$	427	538	27

Table I. API5L Chemical composition. Weight percent.

3.2 Microstructural Properties

The microstructure properties of the material are presented in the fig. 5a for longitudinal direction and 5b for circumferential direction. It shown the presence of ferrite and perlite particles in light and dark tones respectively. It was observed that in both crack extension directions the microstructure shape is banded resulting from the formed material process.

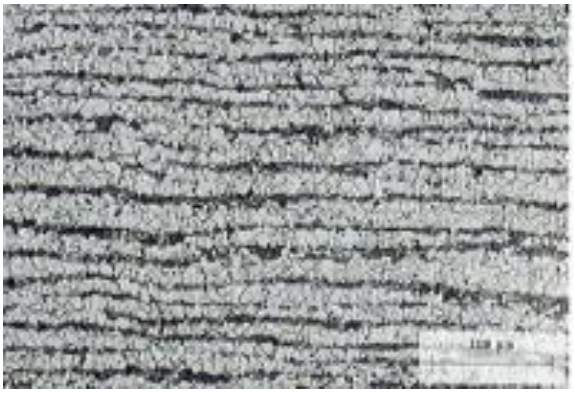

Fig. 5a. Microstructure at longitudinal direction. API-5L steel.

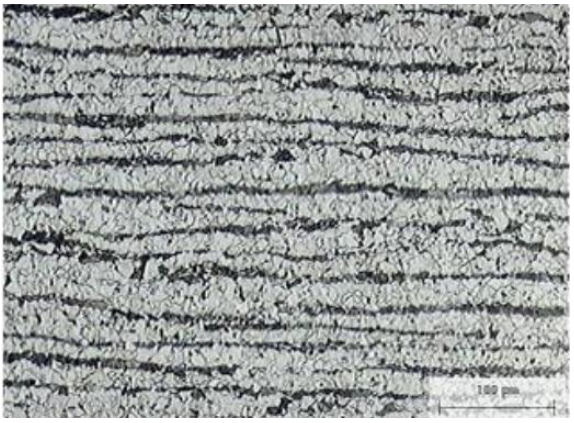

Fig. 5b. Microstructure at circumferential direction. API-5L steel.

3.3 Mechanical Properties

The mechanical characterization of material API-5L was realized by tensile tests according to ASTM E-8. A servohydraulic test machine Shimadzu AG-IS 100 KN of load capacity was used to realize the mechanical tests. Results of yield stress and ultimate stress at longitudinal (L) and circumferential (C) directions are presented in table 2.

Elem / Samp	Fe	C	Si	Mn	P	Cr	Al
1	98.9	0.22	0.05	0.71	0.02	0.01	0.01
2	98.8	0.25	0.06	0.72	0.02	0.01	0.01
3	98.8	0.22	0.05	0.71	0.02	0.01	0.00
Aver.	98.8	0.23	0.05	0.71	0.02	0.01	0.01

Table 2. Mechanical properties API 5L steel.

In order to obtain the yield stress the 0.2% offset method was used like ASTM E-399 specified.

3.4 Test Procedure

Fig 6 shows the specimen crack orientation selected to elaborate the specimens. The Longitudinal and circumferential orientations were considered to propagate the crack.

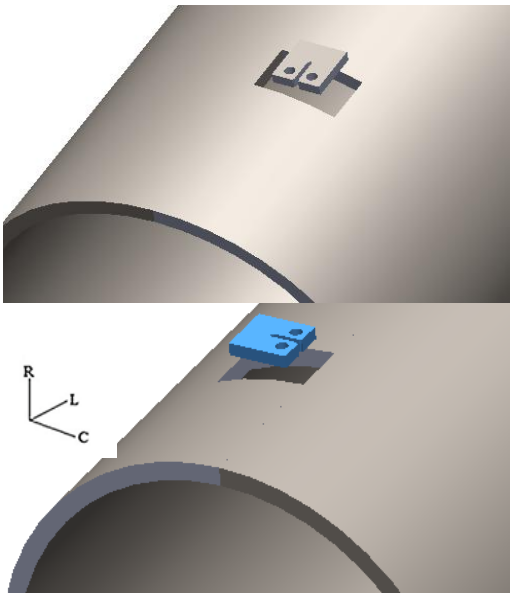

Fig. 6. Longitudinal and circumferential orientations for crack propagation.

Figure 7 shows a compact specimen mounted in MTS-810 machine. The test were realized at room temperature and the specimen was cyclically loaded with a load ratio of R=0.1 and a frequency of 15 Hz. The tested specimens were realized according to ASTM E-399 and its dimensions met the ratio $0.45 \leq \frac{a}{W} \leq 0.55$. The specimen width "w" had a magnitude of 65 mm and the crack length was 33mm. The pre-cracking procedure was induced in all specimens until reach a 1.5 mm crack length. Fracture toughness tests were realized until reach the specimen final fracture.

Fig. 7. Fracture toughness test.

During the fracture toughness test, the crack propagates through the material until reach a critical size. Once the critical size is reached, the final fracture is imminent. Fig. 8 shows the final fracture stage in a compact specimen, at this step exists a great plastic deformation and the surface asperities are large compared with pre-cracking and propagation stages.

Fig. 8. Final fracture stage.

3.5 Recorded Data

The data obtained from the Fracture toughness tests are presented in fig. 9. This image shows the Load vs. COD (Crack Opening Displacement) graphic. The curve presents a typical behavior with a linear pattern at the initial stage of loading and a second stage with large increments in COD and low load increase.

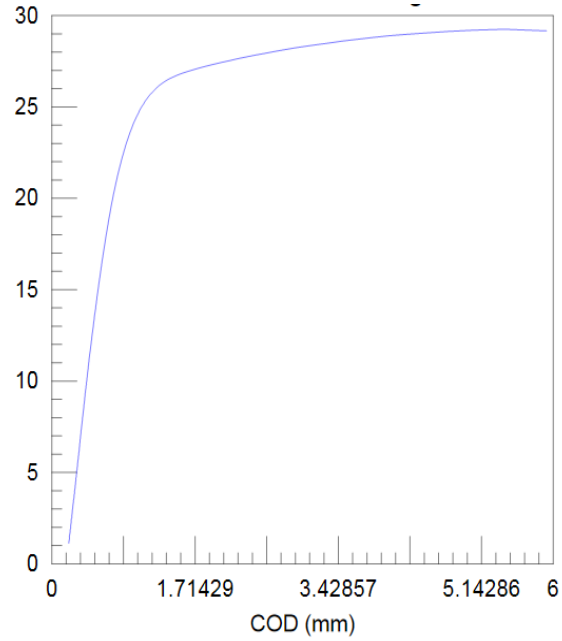

Fig. 9. Load vs. COD curve.

According to ASTM E-399 at "Interpretation of results" section, a straight line tangent to the lineal part of the curve has to be drawn. After that, a secant with 95% of tangent slope is drawn. The intersection point between the curve and the secant is the P_Q point. If the difference between the P_Q point and the maximum load applied (P_{max}), then the test is valid.

Following the above procedure, the data obtained were $P_Q = 26.4\ KN$ and a maximum applied load of $P_{max} = 29.1\ KN$. The load ratio between P_Q and P_{max} was lower than 1.10 and then the test is valid. The Stress intensity factor at "Q" point (K_Q) is calculate as:

$$K_Q = \frac{P_Q}{B\sqrt{W}} f\left(\frac{a}{W}\right)$$

After the test validation, the K_Q obtained from the load applied at point P_Q is considered as K_{IC}.

IV. FINITE ELEMENT ANALYSIS RESULTS

The results obtained by Finite Element Analysis present a maximum stress of 549 MPa located at the crack tip edge. Fig. 10 shows a compact specimen and the stress distribution at the specimen body. The stress distribution around the notch is approximately of 360 MPa and in a small zone near from the crack tip edge the stress concentration reaches the maximum stress.

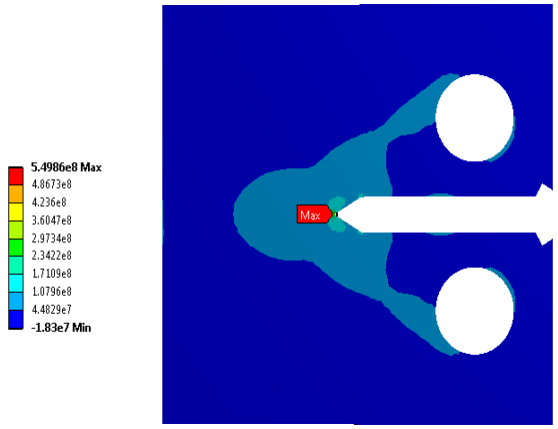

Fig. 10. Stress distribution in Compact specimen

Taking a close image of the crack tip where are concentrated the maximum stresses, is located a small zone around the crack tip edges where the stresses comes around 440 MPa. This zone is known like the plastic deformation zone.

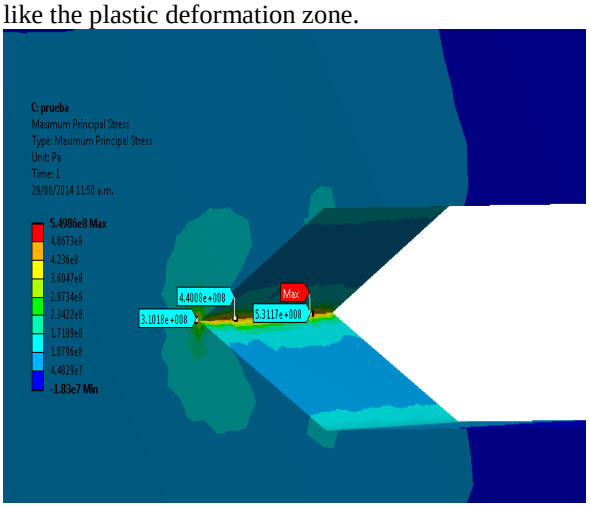

Fig. 11. Close image of crack tip notch.

Submitting the compact specimen to fatigue, the residual life of the element was calculated. The fig 12 presents the life time calculated to a compact specimen cyclically loaded like was described at 2.3 in order to simulate the pre-cracking process. Results shows that the minimum number of cycles from which the material starts to suffering damage is around 2942 cycles. This initial damage is located in a small zone around the crack tip and it is no appreciable.

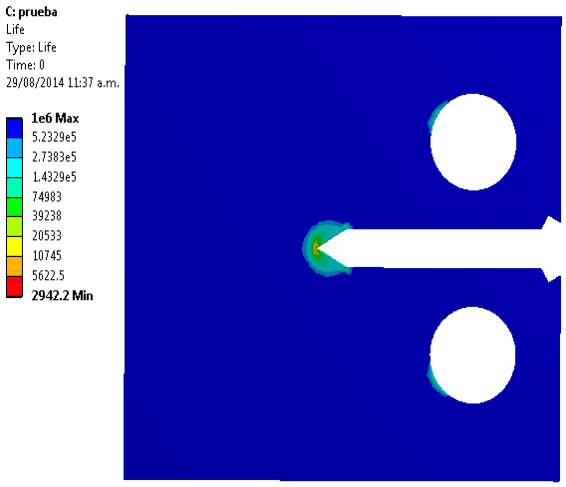

Fig 12. Residual life of the compact specimen

The fig. 17 is a close image of the residual life in fatigue. This image shows the number of cycles from which the damage in the element is bigger than 0.5 mm of extension. This damage occurs at 16 534 cycles, so an appreciable damage in the compact specimen would occur close to 18 to 20 minutes.

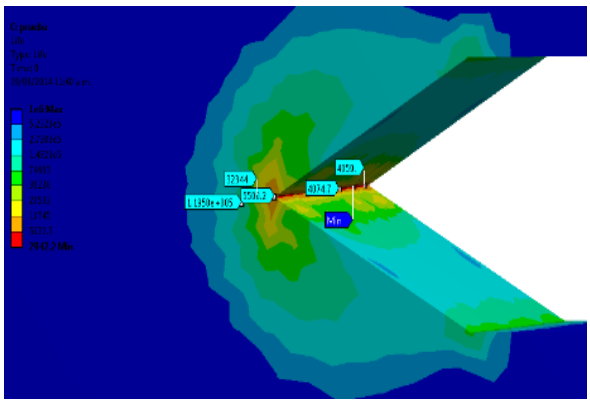

Fig 13. Close image of residual life compact specimen

In order to calculate the stress intensity factor in a compact specimen, a simulated crack was introduced at the notch tip. This crack assume an elliptical shape and extends through all the material thickness to simulate the pre-cracking conditions that are present at the fracture toughness test. Fig 14 presents the location of the simulated crack where a local coordinate system was created to guide the crack orientation. The crack surface is parallel to notch surface.

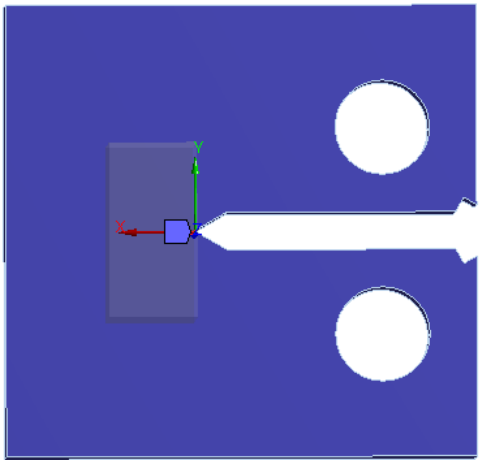

Fig 14. Location of the simulated crack

The simulated crack has a profundity of 1.3 mm. This element has an own meshing area to obtain accurate results. The fig 15 presents an isometric image of the crack inside the compact specimen and it's shape.

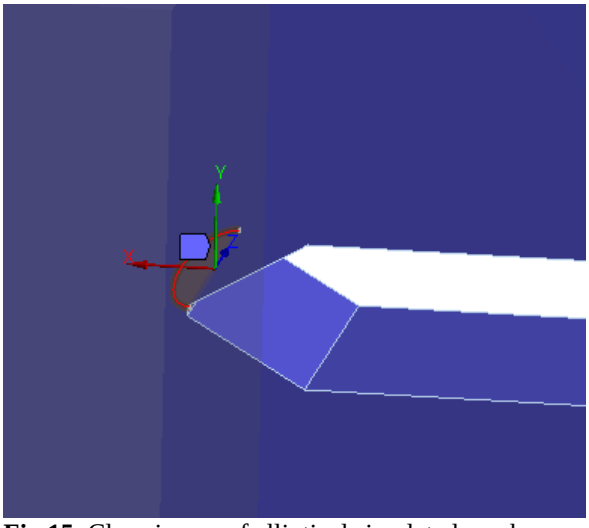

Fig 15. Close image of elliptical simulated crack.

After introducing the simulated crack, the fracture toughness modulus is inserted to calculate the stress intensity factor at mode I (K_{IC}) in the compact specimen. The K_{IC} calculus are performed according to the basis of linear elastic fracture mechanics (LEFM). Fig 16 presents the results of the fracture toughness module introduced and its magnitude. It is observed that the major stress intensity is located at the deeper zone of the inserted crack.

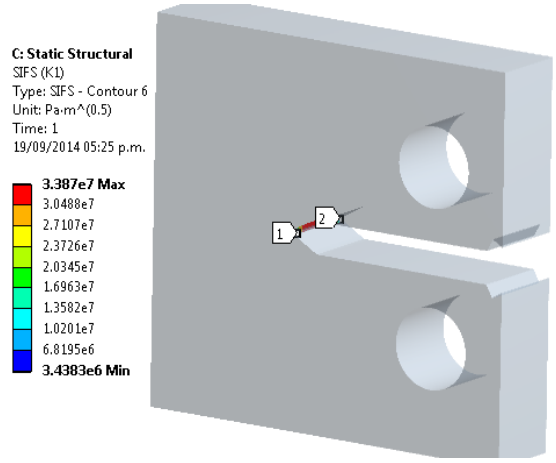

Fig. 17. Stress intensity factor magnitude in compact specimen.

Fig 18 presents the close image of stress intensity factor inside the compact specimen. It shows the lower intensity factors at the outside edges of the crack.

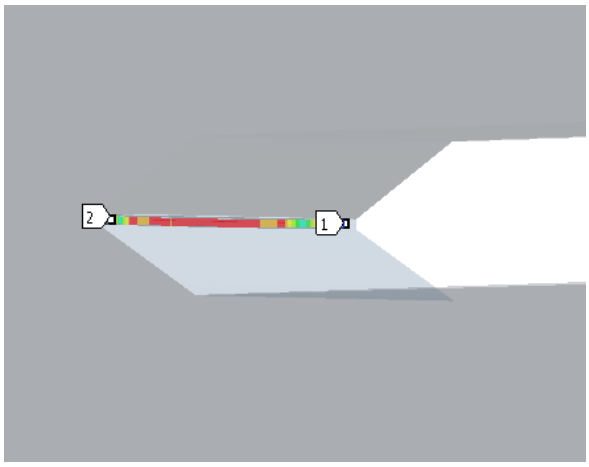

Fig 18. Stress intensity factor at crack tip.

The stress intensity factor simulation was realized in Ansys Workbench 14.5 in linear elastic fracture mechanic basis.

V. CONCLUSION

In this work the fracture toughness characterization was realized in structural steel API 5L according to ASTM E-399 under liner elastic conditions. The compact specimens were used to perform the testing and simulation chapters. The load vs COD curves were obtained and validated according to ASTM E-399 of linear elastic fracture mechanics.

Compact specimens were analyzed by the finite element method using Ansys workbench 14.5 in the fracture module to obtain the K_{IC} parameter. The analysis obtained presented closeness values comparing with the experimental results. According to experimental and simulated results concludes that the finite element analysis provides correct approximation to real fracture toughness values and it could be used to obtain close parameter if the experimental testing couldn't be realized.

ACKNOWLEDGEMENTS

The authors of this work acknowledge to CONACYT institute for the support given.

REFERENCES

[1] González V. J. L. Fracture mechanics (Ed. Limusa Noriega. México, 2004).
[2] Terán G. J., Fracture toughness evaluation in short directions of hydrocarbons pipelines, doctoral diss., IPN. México, 2007
[3] Arana J. L. Fracture mechanics (Ed. Servicio Editorial de la Universidad del País Vasco).
[4] W.E. Anderson and P.C. Paris, "Evaluation of Aircraft Material by Fracture" Metals Engineering Quarterly, vol.1, no.2,p.33. Mav, 1961.
[5] W.E. Anderson and P.C. Paris, A critical analysis of crack propagation laws. Journal of basics engineering trans. ASME.. 1963.
[6] A. J. McEvily and W. Illg, "Th e Rate of Crack Propagation in Two Aluminum Alloys," NASA Technical Note 4394, September, 1958.
[7] H. W. Liu, "Crack Propagation in Thin Metal Sheets Under Repeated Loading," THE JOURNAL OF BASIC ENGINEERING, TRANS. ASME, SeriesD,vol.83,1961,p.23.
[8] N. E. Frostand D. S. Dugdale, "Th e Propagation of Fatigue Crack sin Sheet Specimens," Journal of the Mechanics and Physics of Solids, vol.6, no.2, 1958, p.92
[9] ASTM. Standart Test Method for Linear-Elastic Plane-Strain Fracture Toughness for Metallic Materials, Philadelphia, USA. ASTM E399-12, ASTM Standards Handbook.
[10] ASTM. Standard practice for R-curve determination. American Society Testingand Materials, Philadelphia, USA. ASTM E561-92, ASTM Standards Handbook, 1992.
[11] ASTM. Standard Test Method for Measurement of Fatigue Crack Growth Rates. American Society Testingand Materials, Philadelphia, USA. ASTM E-647. ASTM Standards Handbook.